## REGULAR ARTICLE



# Experimental Investigation for Exploring the Effect of Ca<sup>2+</sup>, Dy<sup>3+</sup> Doping on the Structural and Optical Properties of ZnO NPs

A. Kadari¹,\* <sup>⊠</sup>, M. Cherchab¹, V. Dubey²

Department of Chemistry, Faculty of Matter Sciences, University of Tiaret, 14000 Tiaret, Algeria
 Department of Physics, Bhilai Institute of Technology, 493661 Raipur, New Raipur, India

(Received 19 August 2025; revised manuscript received 21 October 2025; published online 30 October 2025)

Zinc oxide nanoparticles (ZnO NPs) have garnered significant attention from researchers because of their important properties (optical, luminescence, magnetic and electrical properties). Various synthesis methodologies have been documented for crafting of zinc oxide nanoparticles with notable techniques including the co-precipitation method, hydrothermal method, solid state reaction method and sol-gel method. In this present study, pure ZnO, Ca-doped ZnO and Dy-doped ZnO samples were synthesized by sol-gel method. Synthesized nanoparticles were characterized by powder XRD, UV-Vis and FT-IR spectroscopy. The XRD and FT-IR studies of samples confirmed the formation of undoped and doped nanoparticles, with the nanoparticles size calculated using the Debye Scherer's formula falling within the range of 31 and 40 nm. The direct optical band gap ( $E_g$ ) and the Urbach energy ( $E_U$ ) were determined through UV-vis transmittance analysis. Optical band gap energy of 3.377 eV was determined for the pure ZnO nanoparticles in this study. Urbach energies ( $E_U$ ) were observed to range 0.175-1.441 eV. The influence of dopants on some physical properties of elaborated ZnO NPs has been thoroughly analyzed and documented in this research paper.

Keywords: Zinc oxide, Calcium doped ZnO, Dysprosium doped ZnO, Sol-gel, Nanoparticles.

DOI: 10.21272/jnep.17(5).05039 PACS numbers: 61.46.Df, 77.84.Bw, 78.67.Bf

#### 1. INTRODUCTION

In the past decade, metal oxide nanoparticles have garnered substantial attention and are employed in various applications. ZnO stands out as a significant compound semiconductor with a wide direct band gap of 3.37 eV [1]. The unique optical, chemical, acoustical, magnetic and electrical properties of this compound have generated significant research interests [2-4]. ZnO, a wide band gap (3.4 eV) II-IV compound semiconductor, exhibits a stable Wurtzite (B4 type) structure with specific lattice parameters a = 0.325 nm and c = 0.521 nm at standard ambient pressure and temperature conditions. It possesses a hexagonal lattice, falling under the space group P<sub>63mc</sub> with the Pearson symbol of hP4. The compound can be further characterized by two interconnected sub-lattices comprising Zn2+ and O2-Zn ions are surrounded by tetrahedrally arranged O ions, and vice versa. In ZnO, the tetrahedral coordination results in a non-centrally symmetrical structure with polar symmetry along the hexagonal axis, leading to the characteristic piezoelectricity and spontaneous polarization. This structural property is a key factor in the processes of crystal growth, etching and defect generation of ZnO. Apart from Wurtzite phase, ZnO can also crystallize in cubic zinc blende which is only stable when grown on cubic structures [5]. ZnO nanoparticles is extensively used in a variety of industries, such as optical and electrical devices [6],

gas sensors [7], solar cells [8], photo detectors [9], light emitting diodes (LEDs) [10] and laser systems [11]. The preparation of ZnO NPs can be achieved through different methods such as ultrasonic, precipitation, sol-gel, electrodeposition, thermal decomposition of organic precursors, microwave assisted techniques, and so on. Among the various methods available, the sol-gel technique is considered the most effective method for synthesizing ZnO NPs [12-14]. Incorporating dopants can significantly enhance the physical properties of Metal Oxide Nanoparticles (MONPs). Doping of zinc oxide nanoparticles (ZnO NPs) with calcium (Ca2+) and Dysprosium (Dy3+) ions will help in altering the band gap. Physical and chemical characteristics of these ions are similar to Zn2+ ions. It can be also observed here that the ionic radius of Zn<sup>2+</sup> (74 pm), Ca<sup>2+</sup> (100 pm) and Dy<sup>3+</sup> (105 pm) are different making it challenging for dopants ions to easily substituted in the host lattice site and caused a change in the crystal structure. Materials doped with rare-earth ions are promising for their luminescence properties wherein the incorporation of impurities can effectively alter the semiconductor's structure and elicit significant changes in luminescence and optical properties [15]. As a starting point in this work, undoped, calcium and dysprosium doped ZnO samples were successfully prepared by sol-gel method. The structural and optical properties were comprehensively examined and compared. The results indicate that doped samples significantly influence the structural and optical properties at the nano scale level.

2077-6772/2025/17(5)05039(6)

05039-1

https://jnep.sumdu.edu.ua

<sup>\*</sup> Correspondence e-mail: kadariahmed\_14@yahoo.fr

#### 2. EXPERIMENTAL DETAILS

#### 2.1 Sol-gel Synthesis Mechanism

#### 2.1.1 Hydrolysis

 $M\text{-}OR + MOH \rightarrow M\text{-}OH + R\text{-}OH$ 

#### 2.1.2 Condensation

(1) M-OR + OH-M  $\rightarrow$  M-O-M + H<sub>2</sub>O (2) M-OR + M-OH  $\rightarrow$  M-O-M + M-OH

## 2.2 Preparation of ZnO NPs Applying the Sol-Gel Process

The zinc acetate (Zn(CH<sub>3</sub>COO)<sub>2</sub>.2H<sub>2</sub>O, Sigma-Aldrich, USA), NaOH and citric acid (C<sub>6</sub>H<sub>8</sub>O<sub>7</sub>.H<sub>2</sub>O) were used for the syntheses of zinc oxide nanoparticles. All initial chemicals from Sigma Aldrich were of high purity, at 99.99 %. The synthesis process of ZnO NPs Sol-gel involves dissolving 2 gZn(CH<sub>3</sub>COO)<sub>2</sub>.2H<sub>2</sub>O in 100 mL of deionized water to get the precursor solution, followed by the gradual addition of 8 g (dissolved in 15 mL of deionized water) of NaOH solution drop wise. In this step, citric acid (C<sub>6</sub>H<sub>8</sub>O<sub>7</sub>.H<sub>2</sub>O) was used as stabilizer. Using a magnetic stirrer, obtained solution was stirred during 6 h at 60 °C. The focus of this study was on examining the influences of calcium (Ca2+) and dysprosium (Dy3+) impurities on the physical properties of ZnO, so for this reason the same procedure was replicated for the preparation of Ca-doped ZnO and Dy-doped ZnO nanoparticles. Calcium chloride (CaCl<sub>2</sub>.2H<sub>2</sub>O) and dysprosium oxide (Dy<sub>2</sub>O<sub>3</sub>) were used as precursor for the doping steps. White suspended particles were formed which clearly shows the formation of zinc oxide nanoparticles. Subsequently, the washed solution was dried at 100 °C for 24 h followed by calcination at 600 °C for 5 h. Fig. 1 depicts a schematic illustration of the nanoparticles synthesis process.

#### 2.3 Characterization of ZnO NPs

An examination of synthesized nanoparticles involves the utilisation of various analytical methods. The structural parameters of prepared ZnO NPs were determined by employing the MiniFlex 600W powder diffractometer, utilizing CuK $\alpha$  radiation ( $\lambda=1.5406$  Å) in the range from 3 to 90 deg. Optical transmittance in the 200 to 800 nm wavelength was determined using the SHIMADZU (UV-1650-PC) double beam spectrophotometer. Additionally, FT-IR spectra were captured employing the Alpha Bruker FT-IR spectrometer.

## 3. RESULTS AND DISCUSSION

## 3.1 XRD Analysis

The X-ray diffraction (XRD) analysis was conducted using the MiniFlex 600W powder diffractometer with CuK $\alpha$  radiation ( $\lambda$  = 1.5406 Å). The diffraction peaks of XRD were analysed within the range of 2 $\theta$  from 3 to 90°. Fig. 2 illustrates the XRD pattern of ZnO NPs

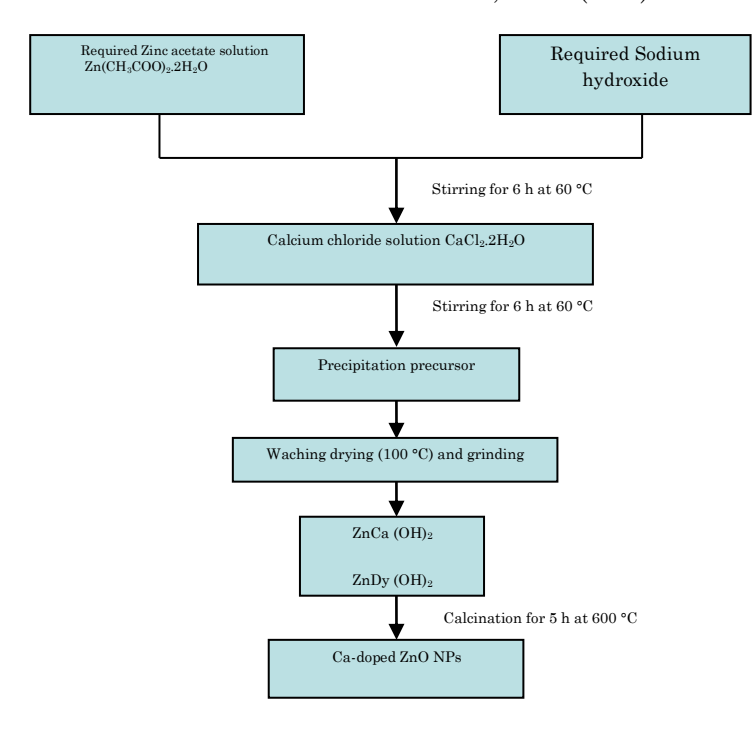
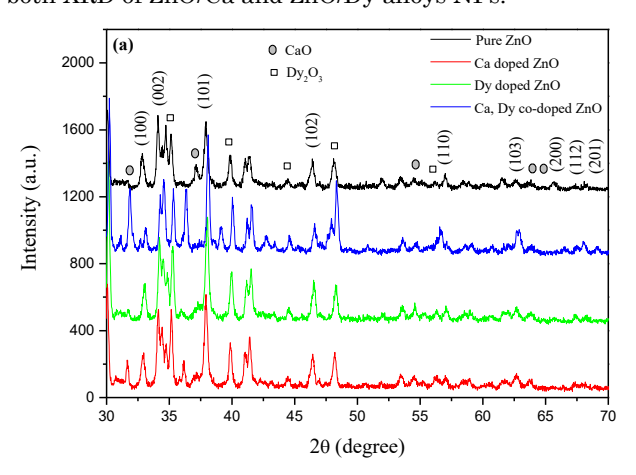


Fig. 1 – Schematic representation for the synthesis of pure ZnO, Ca-doped ZnO and Dy-doped ZnO samples

(pure ZnO, Ca-doped ZnO and Dy-doped ZnO) that have been calcined at a 60 °C for 5 h. Nine diffraction peaks were observed at: 31.68°, 34.39°, 36.27°, 47.48°, 56.52°, 62.89°, 66.35°, 67.92° and 69.05° which corresponds to (100), (002), (101), (102), (110), (103), (200), (112) and (201) Miller planes. The obtained data aligns with previously reported XRD data of ZnO NPS (JCPDS File Number 36-1451), confirming the formation of pure and doped ZnO nanoparticles [16,17]. On the other hand, the good incorporation of Ca2+ and Dy3+ ions in ZnO lattice, was confirmed by the presence of CaO and Dy2O3 oxides in the XRD patterns following to the JCPDS cards No. 78-0649 (CaO) [18.19] and JCPDS cards No. 22-0612 (Dv<sub>2</sub>O<sub>3</sub>) [20-23] respectively. In addition, the XRD patterns for ZnO/Ca and ZnO/Dy alloys nanoparticles are displayed in Fig. 2 (b). From the figure it is clearly revealed that these two diffractograms are completely different as compared with the ZnO NPs doped Ca<sup>2+</sup> and Dy<sup>3+</sup> ions. The shift of the XRD peaks indicates the alloys formation between metallic phases; also, the pure ZnO peaks are note found in both XRD of ZnO/Ca and ZnO/Dy alloys NPs.



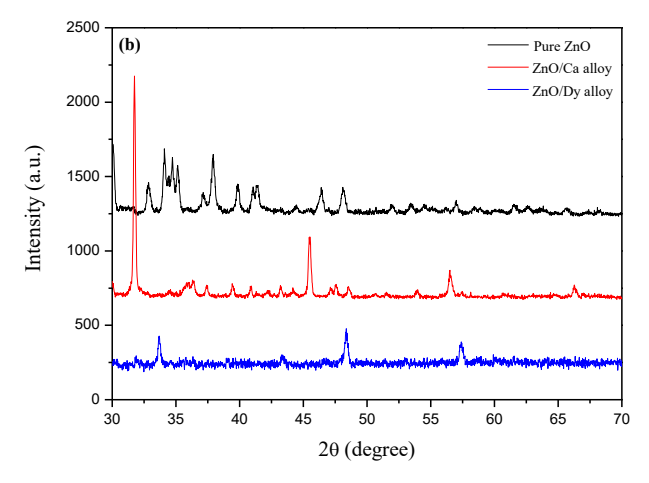


Fig. 2 - XRD pattern of the synthesized nanoparticles: (a) Pure ZnO, Ca, Dy-doped ZnO, (b) ZnO/Ca and ZnO/Dy alloys

Even after the addition of Ca and Dy-ions, the crystal structure is not preserved. This suggests that these ions have replaced Zn sites leading to alterations in the crystal structure. The reason for this is that the ionic radii of Ca<sup>2+</sup> (100 pm) and Dy<sup>3+</sup> (105 pm) are not equivalent to that of  $Zn^{2+}$  (74 pm).

Equations (1), (2) and (3) were utilised to calculate the lattice parameters and the unit cell volume (V). Observations show slight variations in the calculated lattice parameter values between the pure and doped

samples, indicating that the preservation of hexagonal Wurtzite structure even after doping ZnO with Ca and Dy ions.

$$a = \frac{\lambda}{\sqrt{3}\sin\theta},$$

$$c = \frac{\lambda}{\sin\theta}$$
(2)
$$V = \frac{\sqrt{3}a^{2}c}{2}$$
(3)

$$c = \frac{\lambda}{\sin \theta} \tag{2}$$

$$V = \frac{\sqrt{3}a^2c}{2} \tag{3}$$

The Debye Scherrer's formula was employed to determine the average size of synthesized pure ZnO, Cadoped ZnO and Dy-doped ZnO nanoparticles; this formula is given below, the calculated crystallite sizes of ZnO NPs were tabulated in Table 1.

$$D = \frac{K \times \lambda}{\beta \times \cos \theta} \tag{4}$$

where: D – represents the average crystallite size; K – stands for the Sherrer's constant (0.89);  $\lambda$  – denotes the X-ray wavelength (1.5406 Å);  $\beta$  – represents the full width at half maximum (FWHM) of the diffraction peak in radians;  $\theta$  – indicates the Bragg angle.

The dislocation density,  $\delta$  was calculated using the formula  $[\delta = 1/D^2]$  and the results were listed below.

Table 1 - Lattice parameters, average crystallite sizes and the dislocation density values of pure ZnO, Ca-doped ZnO and Dydoped ZnO NPs

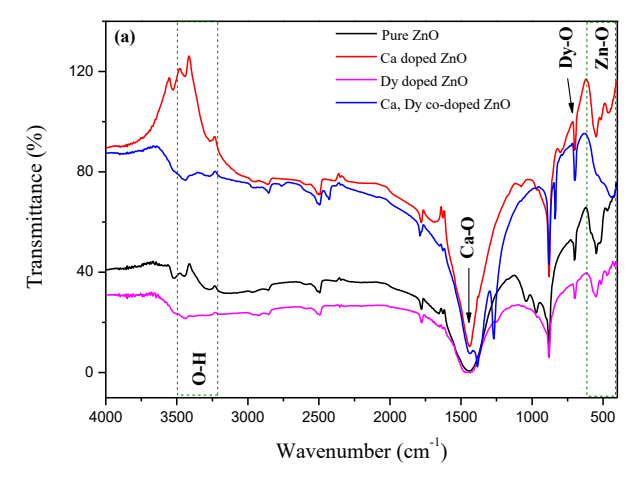
Sample	a (Å)	b Å)	c/a	$V(\mathrm{\AA}^3)$	$2\theta$ (deg)	$\beta$ (deg)	D (nm)	$\delta$ (line/m <sup>2</sup> )
ZnO	3.434	5.941	1.73	60.672	30.046	0.261	31.511	$1.01 \times 10^{15}$
Ca-doped ZnO	3.434	5.941	1.73	60.672	30.044	0.251	32.767	$9.31 \times 10^{14}$
Dy-doped ZnO	3.424	5.924	1.73	60.147	30.135	0.246	33.440	$8.94 \times 10^{14}$
Ca, Dy-doped ZnO	3.415	5.908	1.73	59.669	30.218	0.216	38.092	$6.89 \times 10^{14}$
ZnO/Ca Alloy	3.255	5.632	1.73	51.676	31.735	0.203	40.679	$6.04 \times 10^{14}$
ZnO/Dy Alloy	3.545	6.134	1.73	66.758	29.079	0.208	39.454	$6.42 \times 10^{14}$

#### 3.2Fourier Transform Infrared Spectroscopy (FT-IR)

Fourier Transform Infrared Spectroscopy (FT-IR) was utilized to analyse the surface chemistry of the synthesized ZnO nanoparticles using an Alpha Bruker FT-IR spectrometer. This technique was applied to identify the surface functionality and vibrational modes of the inorganic core of the prepared additives. Functional groups attached to the surface of NPs were detected in the range of 4000-400 cm<sup>-1</sup>. The formation and purity of ZnO NPs and the good incorporation of their dopants were further validated through FT-IR spectra as shown in Fig. 3(a) and (b). The peak at 400-600 cm<sup>-1</sup> corresponds to the ZnO [24], whereas the broad maximum observed in the range 3200-3550 cm<sup>-1</sup> is due to the stretching vibration of hydroxyl compounds (adsorbed water) [17]. As anticipated, the IR spectrum of the prepared CaO powder exhibits a very strong absorption band at around 1430 cm<sup>-1</sup>, and two sharp bads centred at 1430, 880, and 713 cm<sup>-1</sup> resulting from the stretching modes of carbonate ion [24]. An absorption peak with significant strength observed at approximately 560 cm<sup>-1</sup> can be attributed to the vibration of the Dy-O bond, as stated in reference [25].

#### 3.3 UV-Visible Spectroscopy

Examining the impact of doping on the optical characteristics of synthesized ZnO, Ca-doped ZnO and Dy-doped ZnO nanoparticles; a UV-Visible transmittance study is a valuable tool for this purpose. These nanoparticles were analysed using the UV-Vis Spectroscopy, utilising the SHIMADZU (UV-1650-PC)



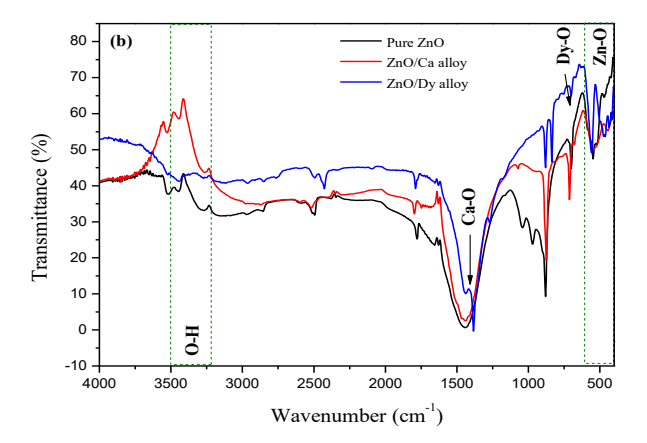


Fig. 3 - The FT-IR spectra of the synthesized nanoparticles: (a) Ca, Dy-doped ZnO (b) ZnO/Ca and ZnO/Dy alloys

double beam spectrophotometer, between 200 and 800 nm at room temperature. It is interesting to note that the optical parameters (absorbance and transmittance) depend on particle size, impurity centers, band gap and lattice parameters. The optical transmittance spectra of synthesized ZnO, Ca-doped ZnO and Dy-doped ZnO NPs were shown in Fig. 4, revealing a common minimum transmittance around 325 nm; beyond this value the transmittance is increased.

The Optical band gap energy of ZnO NPs was found by employing Tauc's plot method and the results were tabulated in Table 2, confirming the semiconductive nature of the synthesized nanoparticles indicating that they are wide band gap materials. This method uses the formula [26]:

$$(\alpha h \nu)^{1/m} = B(h \nu - E_{g}) \tag{4}$$

where: h – the Planck's constant (h = 6.63  $\times$  10<sup>-34</sup>  $m^2 \cdot kg/s$ ; B – the band tailing parameter;  $\nu$  – the frequency (Hz);  $E_g$  – is the band gap energy (eV); m – represents the type of electronic transition.

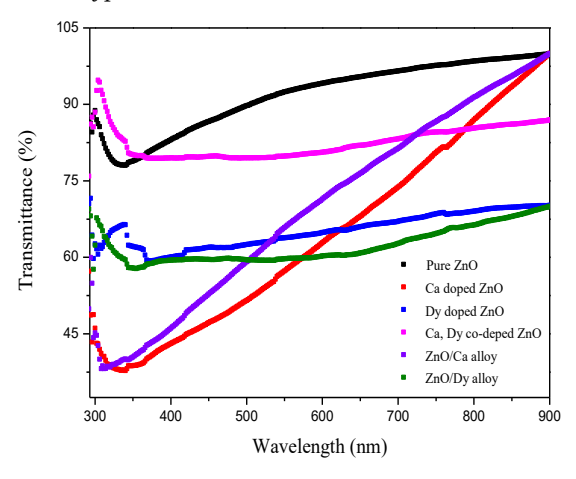
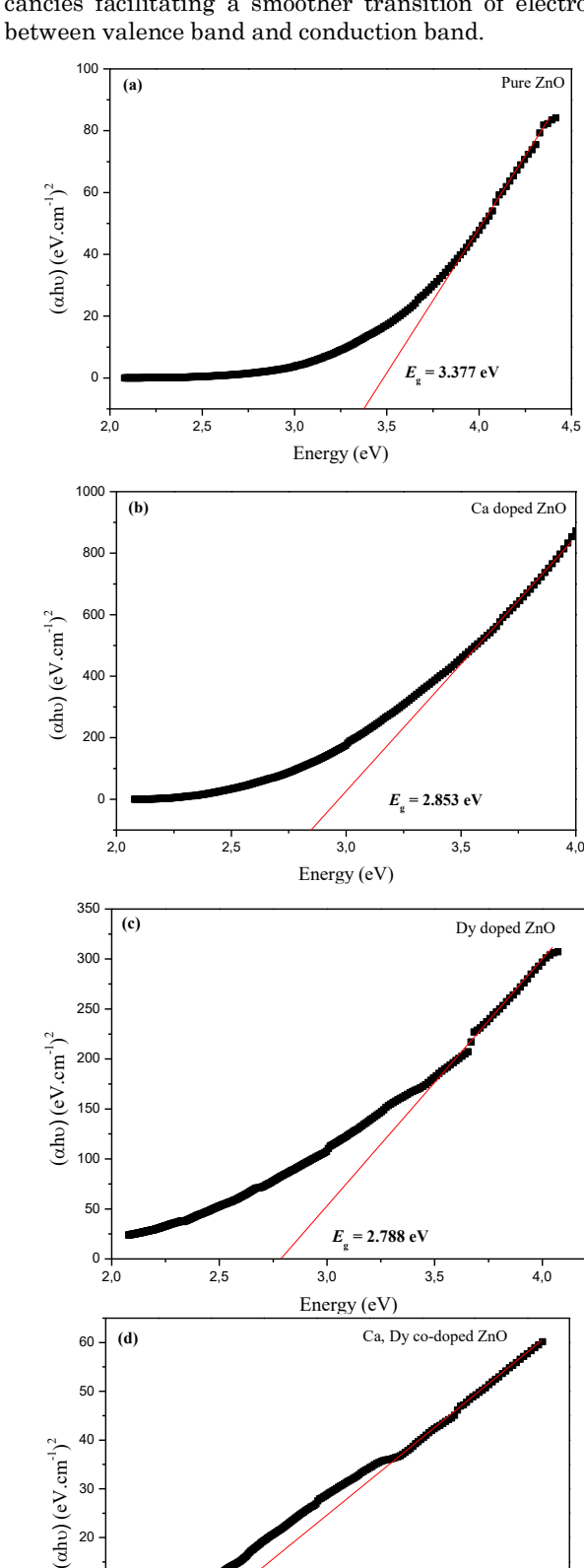


Fig. 4 - Optical transmittance spectra of ZnO, Ca-doped ZnO and Dy-doped ZnO samples

The optical band gap energy calculated for the pure ZnO nanoparticles is 3.377 eV. On doping our synthesized nanoparticles (ZnO NPs) with Ca and Dy ions; the calcium and dysprosium atoms enters into the crystalline structure of ZnO leading to a reduction of the

band gap from 3.377 eV to 2.222 eV. This modification could be attributed to the presence of the oxygen vacancies facilitating a smoother transition of electrons



 $E_{\rm g} = 2.222 \text{ eV}$ 

3,0

Energy (eV)

3,5

4,0

2,5

30

20

2,0

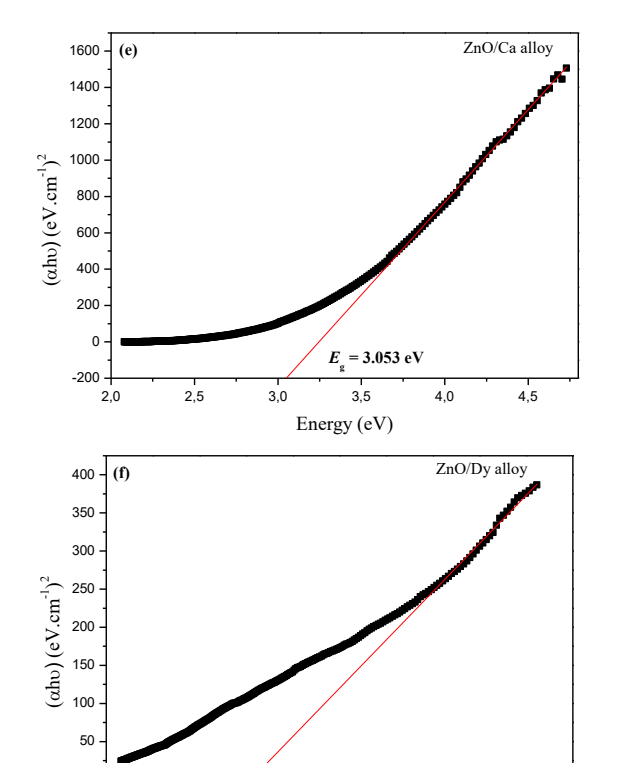


**Fig. 5** – Optical band gap energy of: (a) Pure ZnO, (b) Cadoped ZnO, (c) Dy-doped ZnO, (d) Ca, Dy co-doped ZnO, (e) ZnO/Ca alloy and (f) Dy/ZnO alloy

3,0

 $E_{-} = 2.689 \text{ eV}$ 

Energy (eV)

3,5

4.0

 ${\bf Table~2-Optical~band~gap~energy~and~Urbach~energy~of~pure~ZnO,~Ca-doped~ZnO~and~Dy-doped~ZnO~samples } \\$ 

Sample	$E_{\mathrm{g}}$ (eV)	$E_{\mathrm{U}}$ (eV)
ZnO	3.377	1.441
Ca-doped ZnO	2.853	0.823
Dy-doped ZnO	2.788	0.175
Ca, Dy-doped ZnO	2.222	0.211
ZnO/Ca Alloy	3.053	1.072
ZnO/Dy Alloy	2.689	0.187

Furthermore, the determination of Urbach energy  $(E_{\rm U})$  of the ZnO nanoparticles was conducted by analysing the curves of  ${\rm Ln}a$  as a function of photon energy hv (Fig. 6). Similar to the optical gap, the Urbach energy  $(E_{\rm U})$  is intricately linked to the disorder present in the synthesized nanoparticles. This relationship is mathematically expressed as indicated in reference [28]. The specific values of the Urbach energy can be found in Table 2.

### REFERENCES

- A. Chelouche, T. Touam, D. Djouadi, A. Aksas, *Optik* 125, 5626 (2014).
- N.H. Deepthi, R.B. Basavaraj, S.C. Sharma, J. Revathi, S. Ramani, H.N. Sreenivasa, J. Sci.: Adv. Mater. Dev. 3, 18 (2018).
- 3. S. Munjal, N. Khare, AIP Conf. Proc. 1724, 20092 (2016).
- 4. M. Wang, RSC Adv. 6, 36264 (2016).
- K. Rekha, M. Nirmala, MG. Nair, A. Anukaliani, *Physica* B 405, 3180 (2010).

$$A = A_0 \exp\left(\frac{h\upsilon}{E_U}\right) \tag{5}$$

$$\alpha = \alpha_0 \exp\left(\frac{h\upsilon}{E_U}\right) \tag{6}$$

where,  $A_0$  and  $\alpha_0$  are constants and  $E_{\rm U}$  is the Urbach energy.

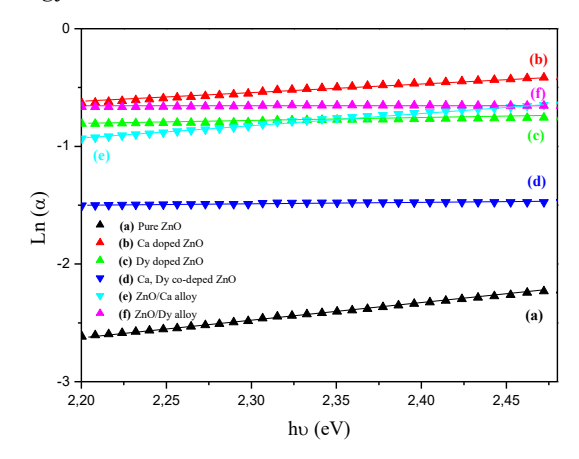


Fig. 6 – Ln (a) versus ( $h\nu$ ) of pure ZnO, Ca-doped ZnO and dydoped ZnO samples

#### 4. CONCLUSION

In this paper pure ZnO, Ca-doped ZnO and Dy-doped ZnO nanoparticles were synthesized by Sol-gel method and then calcined for 5 h at 600 °C. Different characteristic like XRD, FT-IR and UV-Vis spectroscopy were analysed. The XRD pattern was employed to identify the crystal structure, phase purity and grain size of the synthesis nanoparticles. The average size of the nanoparticles was determined using Debye Scherer's formula, resulting in sizes between 31 and 40 nm. The band gap energy for the pure ZnO nanoparticles is 3.377 eV. Urbach energies ( $E_{\rm U}$ ) fell within the range 0.175 eV-1.441 eV. In conclusion, we are confident that our findings present promising prospects for future exploration.

### **AKNOWLEDGEMENTS**

This work was supported by the Algerian Ministry of Higher Education and Scientific Research and the General Directorate for Scientific Research and Technological Development (DGRSDT).

- M.H. Huang, S. Mao, H. Feick, H. Yan, Y. Wu, H. Kind, E. Weber, R. Russo, P. Yang, *Science* 292, 1897 (2001).
- M.C. Carotta, A. Cervi, V.D. Natale, S. Gherardi, A. Giberti, V. Guidi, D. Puzzovio, B. Vendemiati, G. Martinelli, M. Sacerdoti, D. Calestani, A. Zappettini, M. Zha, L. Zanotti, Sensor. Actuat. B: Chem. 137, 164 (2009).
- M. Krunks, A. Katerski, T. Dedova, I. Acik, A. Mere, Sol. Energy Mater. Sol. C. 92, 1016 (2008).
- 9. C.L. Hsu, S.J. Chang, Y.R. Lin, P.C. Li, T.S. Lin, S.Y. Tsai,

- T.H. Lu, I.C. Chen, Chem. Phys. Lett. 416, 75 (2005).
- D. Wang, H. Zhuang, C. Xue, J. Shen, H. Liu, *Mater. Lett.* 63, 370 (2009).
- 11. L.E. Li, L.N. Demianets, Opt. Mater. 30, 1074 (2008).
- 12. M. Kahouli, A. Barhoumi, A. Bouzid, A. Al-Hajry, S. Guermazi, *Superlattice. Microst.* **85**, 7 (2015).
- 13. D. Raoufi, Renew. Energy 50, 932 (2013).
- S.S. Kumar, P. Venkateswarlu, V.R. Rao, G.N. Rao, *Int. Nano Lett.* 3, 30 (2013).
- Z. Ben Ayadi, L. El Mir, K. Djessas, S. Alaya, *Nanotechnology* 18, 445702 (2007).
- A.M. Bayader, A. Ghatea, M.H. Risan, *Iraqi J. Nanotechnol.*, Synth. Appl. 4, 93 (2023).
- Z. Aalami, M. Hoseinzadeh, P.H. Manesh, A.H. Aalami,
   Z. Es'haghi, M. Darroudi, A. Sahebkar, H.A. Hosseini,
   Heliyon 10, 24212 (2024).
- H. Huili, A. Mater, B. Grindi, G. Viau, A. Kouki, L.B. Tahar, *Arab. J. Chem.* 12, 489 (2019).
- P. Prajapati, S. Shrivastava, V. Sharma, P. Srivastava, V. Shankhwar, A. Sharma, S.K. Srivastava, D.D. Agarwal,

- Res. Eng. 18, 101063 (2023).
- N.D. Sharma, J. Singh, S. Dogra, D. Varandani, H.K. Poswal, S.M. Sharma, A.K. Bandyopadhyay, *J. Raman Spectroscopy* 42, 438 (2010).
- M. Chandrasekhar, D.V. Sunitha, N. Dhananjaya, H. Nagabhushana, S.C. Sharma, B.M. Nagabhushana, C.Shivakumara, R.P.S. Chakradhar, *J. Lumin.* 132, 1798 (2012).
- 22. B.M. Abu-Zied, A.M. Asiri, J. Rare Earths 32, 259 (2014).
- S. Balaji, S. Aravindhan, S. Srinivasan, *Mater. Lett.* 363, 136200 (2024).
- 24. F.A. Miller, C.H. Wilkins, Anal. Chem. 24, 1253 (1952).
- M.S. Niasari, J. Javidia, F. Davar, *Ultrason. Sonochem.* 17, 870 (2010).
- A.Z. Johannes, R.K. Pingak, M. Bukit, *IOP Conf. Ser.: Mater. Sci. Eng.* 823, 12030 (2020).
- K.J. Archana, A.C. Preetha, K. Balasubramanian, Opt. Mater. 127, 112245 (2022).

# Експериментальні дослідження для вивчення впливу легування Ca<sup>2+</sup>, Dy<sup>3+</sup> на структурні та оптичні властивості НЧ ZnO.

## A. Kadari<sup>1</sup>, M. Cherchab<sup>1</sup>, V. Dubey<sup>2</sup>

<sup>1</sup> Кафедра хімії, Факультет наук про речовину, Університет Тіарет, 14000 Тіарет, Алжир <sup>2</sup> Факультет фізики, Технологічний інститут Бхілай, 493661 Райпур, Нью-Райпур, Індія

Наночастинки оксиду цинку (НЧ ZnO) привернули значну увагу дослідників через їхні важливі властивості (оптичні, люмінесцентні, магнітні та електричні). Були задокументовані різні методології синтезу для виготовлення наночастинок оксиду цинку з відомими методами, включаючи метод спільного осадження, гідротермальний метод, метод реакції твердого тіла та золь-гель метод. У цьому дослідженні чистий ZnO, легований Ca ZnO та ZnO, легований Dy, були синтезовані золь-гель методом. Синтезовані наночастинки були охарактеризовані порошковою XRD, UV-Vis та FT-IR спектроскопією. Дослідження XRD та FT-IR зразків підтвердили утворення нелегованих і легованих наночастинок, причому розмір наночастинок, розрахований за формулою Дебая Шерера, знаходиться в діапазоні 31 і 40 нм. Пряму оптичну заборонену зону ( $E_g$ ) та енергію Урбаха ( $E_U$ ) визначали за допомогою аналізу пропускання в УФ-виді. У цьому дослідженні для чистих наночастинок ZnO було визначено енергії оптичної забороненої зони 3,377 еВ. Спостерігалося, що енергії Урбаха ( $E_U$ ) коливаються в діапазоні 0,175-1,441 еВ. Вплив легуючих добавок на деякі фізичні властивості розроблених наночастинок ZnO було ретельно проаналізовано та задокументовано в цій дослідницькій статті.

Ключові слова: Оксид цинку, Легований кальцієм ZnO, Легований диспрозієм ZnO, Золь-гель, Наночастинки.